UNIVERSIDAD NACIONAL DE COLOMBIA
SEDE MEDELLÍN
FACULTAD DE MINAS

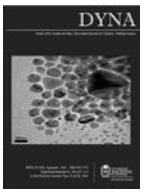

DYNA
http://dyna.medellin.unal.edu.co/

Facile one-pot synthesis of uniform silver nanoparticles and growth mechanism

Daniel Ramirez & Franklin Jaramillo

Centro de Investigación, Innovación y Desarrollo de Materiales-CIDEMAT, Universidad de Antioquia - UdeA, Medellín, Colombia.
estiben.ramirez@udea.edu.co, franklin.jaramillo@udea.edu.co

Received: January 29th, 2015. Received in revised form: November 20th, 2015. Accepted: March 30th, 2016.

Abstract
Size controlled silver nanoparticles were obtained via chemical reduction using one-pot synthesis. Differently from other reported methods for silver nanoparticles, 1-octanol was used as both solvent and reduction agent, oleylamine and oleic acid acted as capping agents and silver nitrate was used as the metal precursor. Ultraviolet-visible and Raman spectroscopy were used to monitor the in situ growth of the nanoparticles and to corroborate the oxidation of the alcohol to caprylic acid. X-ray diffraction (XRD) and transmission electron microscopy (TEM) served to find the size and shape of the nanoparticles. It was found that the temperature used and the reagents proportions were appropriated to produce silver nanoparticles. A growth mechanism was proposed including the formation of silver carboxylates as an intermediate step of the reaction. As a systematic use of oleic acid, we could observe that a higher concentration of this capping agent led to smaller and more homogenous nanoparticles, less than 5nm in size.

Keywords: silver nanoparticles, nanoparticles growth, capping agents.

Fácil síntesis en un paso y mecanismo de formación de nanopartículas de plata

Resumen
En este trabajo se obtuvieron nanoparticulas de plata por la ruta de reducción química usando síntesis en un paso. Diferente a otros métodos reportados para nanoparticulas de plata, se usó 1-octanol como solvente y agente reductor, oleilamina y ácido oleico como agentes estabilizantes, mientras que el precursor del metal fue nitrato de plata. El crecimiento de las nanopartículas fue monitoreado por espectroscopia de absorción ultravioleta-visible y Raman, lo cual corroboró la oxidación del alcohol a ácido caprilico. Los ensayos de difracción de rayos X y microscopia electrónica de transmisión permitieron conocer la forma y el tamaño de las nanopartículas. Se encontró que la temperatura y los reactivos empleados fueron apropiados para producir nanopartículas de plata. Se formaron carboxilatos de plata como un paso intermedio en la reacción. Finalmente, el incremento en la concentración de ácido oleico permitió la obtención de nanopartículas de plata de menos de 5nm.

Palabras clave: nanopartículas de plata, crecimiento, agentes estabilizantes.

1. Introduction

Silver nanoparticles are very attractive due to their remarkable size and shape-dependent electronic and optical properties [1,2]. Hence, they have been used in a broad range of fields which include catalysis, photonics and surface-enhanced Raman scattering (SERS) [3-10]. It has also been demonstrated that they have highly effective bactericide properties related to the continuous release of silver ions, and therefore they have become one of the most commercialized nanotechnology products in the area of health care; i.e., for bandages, clothing, and cosmetics [11].

The absorption spectrum of silver nanoparticles is sharp and strong, a feature which is ascribed to the so called surface

How to cite: Ramirez. D. & Jaramillo. F. Facile one-pot synthesis of uniform silver nanoparticles and growth mechanism DYNA 83 (198) pp. 165-170, 2016.

DYNA 83 (198), pp. pp. 165-170, Septiembre, 2016. Medellín. ISSN 0012-7353 Printed, ISSN 2346-2183 Online
DOI: http://dx.doi.org/10.15446/dyna.v83n198.48707

plasmons, which consists in the excitation of collective electron oscillations, in response to an electromagnetic field [12]. The optical properties of silver nanoparticles are dictated by the morphological parameters, such as size and shape; hence it is crucial to be able to control these parameters [13].

Many strategies have been developed for the preparation of silver nanoparticles. Mehta S.K. et al [14] prepared silver nanoparticles with controlled shapes and size in homogeneous aqueous solutions using silver nitrate and different saccharides in a micellar media with sodium dodecyl sulfate as surfactant. More complex methods have also been developed, like the use of gamma radiation known as the radiolytic reduction method, in which an aqueous solution of the silver precursor (commonly silver nitrate) is irradiated with gamma rays in order to generate reactive species capable of reducing silver ions Ag+ into zero-oxidation state silver atoms (Ag^0) [15,16]. Tri-sodium citrate, tannic acid and silver nitrate have also been used [17], but some other methods require the usage of uncommon silver tetradecanoate as a precursor reagent [18]. One of the most common reducing agents for the synthesis of nanoparticles is 1,2-hexadecanediol [19,20], and other less expensive capping and reducing agents like liquid paraffin [21] have also been used. In this case, 1-octanol, which is a very common and available solvent, is explored both as a solvent and a reducing agent.

2. Experimental methods

In order to fulfill the requirements of a standard, high purity (>99.8%) silver nitrate and 1-octanol were purchased from Merck, Oleic Acid (90%) from Alfa Easer and technical grade oleylamine (70%) from Sigma-Aldrich. All these reagents were used without any further purification.

2.1. Synthesis of silver nanoparticles

Silver nanoparticles were obtained by a facile method via one-pot synthesis. The reagents used are described in Table 1. Changes were made to the quantity of Oleic acid rather than the quantity of oleylamine or 1-octanol because of this reagent's lower cost. In order to synthesize nanoparticles with uniform sizes, a "hot injection" rather than "heating up" method was adopted as proposed by Chen Y. et al [22]. 1-octanol, oleylamine and oleic acid were added in a 100 mL two-neck flask, and the mixture was heated to 180°C under magnetic stirring. Upon reaching the set temperature, $AgNO_3$ was added and the reaction continued and at the same time aliquots were taken at different times and cooled in an ice bath in order to follow the kinetic by Raman and UV-vis absorbance measurements. The resulting dark brown solution was cooled down to room temperature, and the product was precipitated by adding ethanol to the solution and collected by centrifugation at 5000 rpm for 5min, which was further purified by washing with ethanol 2–3 times. Final products were re-dispersed in hexane for later use and analysis.

Table 1.
Reagents used in the synthesis.

Nomenclature	$AgNO_3$ (mg)	Oleic acid (ml)	Oleylamine (ml)	1-Octanol (ml)
Ag1	203	2.0	2.5	30
Ag2	203	3.0	2.5	30
Ag3	203	4.0	2.5	30

Source: The authors

2.2. UV–Vis absorption spectrophotometry

The UV-vis absorption spectra were taken at room temperature on a UV-vis spectrophotometer Cary 100 from Varian Inc, with a variable wavelength between 300 and 800 nm using a glass cuvette with an optical path of 1 cm.

2.3. X-ray diffraction (XRD)

The X-ray powder diffraction (XRD) pattern was recorded using a PANalytical X-ray diffractometer with Cu Kα radiation (1.5406Å). Samples for measurement were prepared by dropping silver colloids (dispersion in hexane) on the Mylar grid and allowing them to dry at room temperature. The scan step size was 0.0525, ranging from 20 to 90º with a time per step of 64s.

2.4. Micro-Raman spectroscopy

Raman spectra of the samples were recorded using a Horiba Yvonjobin dispersive micro-Raman spectrophotometer. A 785nm laser for the excitation radiation was used. All the spectra were collected in the range 3700–100cm^{-1}.

2.5. Transmission electron microscopy (TEM)

Transmission electron microscopic images were obtained on a FEI Tecnai TEM. Samples for the TEM were dispersed in hexane and deposited on an amorphous carbon film-coated copper grid followed by natural evaporation at room temperature.

3. Results

Fig. 1 shows a picture of the resulting nanoparticles dispersed in hexane after being purified. The brown color is very characteristic of the colloidal dispersion. Visual monitoring was carried out for 2 months and no color change or sedimentation was observed, indicating that the particles were very stable in this solvent.

3.1. Growth process of silver nanoparticles: UV-Vis and Raman spectra

2 mL aliquots of the reacting solution were deposited into test tubes at different times (2, 10, 30, 60 and 120min) and then immediately cooled in ice water to stop the reaction. To carry on the optical spectra of the nanodispersions, 20µL of each aliquot were diluted into 3mL of ethanol.

Figure 1. Picture of silver nanoparticles dispersed in hexane.
Source: The authors

The evolution of the growing silver nanoparticles was monitored by their change of the UV-visible spectrum. Fig. 2a shows the resultant absorbance spectra for Ag2. A very characteristic absorption peak could be observed around 460nm. We can see that the absorbance increased rapidly in just 2 minutes, indicating a higher concentration of silver nanoparticles; after 2 hours the change was not significant, because all particles were already formed. A blue shift was found while the reaction occurred, which is consistent with other reports [23]. As the position of the peak is very dependent on the nanoparticles' size [21] the 460nm peak is not the real one associated to the plasmon resonance of the particles, because they were not well dispersed in the samples taken from the reacting solution (aggregates absorb at higher wavelengths). Lower peak positions were obtained after purification and dispersion in hexane (See Fig. 5).

The two well-defined processes associated with the nucleation and growth of the particles can be observed in Fig. 2b. These are similar to those proposed by Lamer and Dinegar [24] who studied the variation of the solute concentration as a function of time. Nucleation implies an increase in the number of scattering centers (number of particles) for a given system, and therefore gives an increase in the scattered intensity. In contrast, the growth of particles is associated with a decrease of the scattered intensity since the observation window corresponds to the diffraction of smaller particles that are disappearing during the growth process or dissolution of the unstable nucleus. It is consistent with the mechanism of the reduction of Ag^{+} ions and the association of Ag^{0} atoms to produce metallic Ag particles as proposed by several authors [14,25,26].

Raman measurements were also carried out in order to understand the evolution of the reaction. It was not possible to find a clear reported position band for the absorption of silver nanoparticles in the literature, but it is known that silver presents a lattice vibrational mode between 50 and 300cm^{-1} depending on whether it is present as oxide, nitrate, chloride or as some other compound [26]. Nevertheless, as a reference we decided to use a 99.99% pure silver wire to compare with

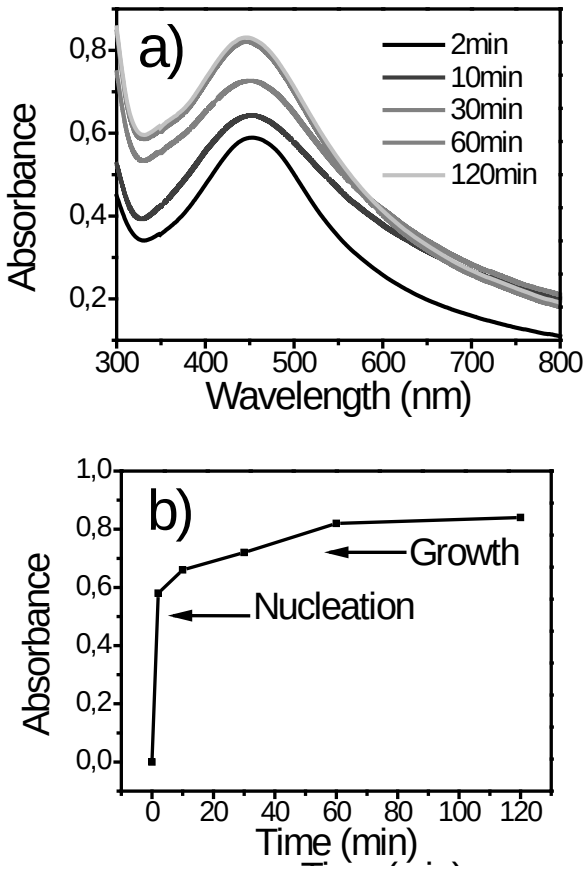

Figure 2. UV-Vis absorption spectra of the Ag2 reaction mixture.
Source: The authors

Table 2.
Raman assignment.

Raman shift (cm^{-1})	Assignment [27, 28]
244	Ag lattice vibrational mode of silver standard
270	Ag lattice vibrational modes of silver nanoparticles
1302	C-O stretching
1388	COO stretching
1438	CH_2 scissoring
1658	C=O stretching

Source: The authors

the position for the metallic silver. The observed bands were found to be 244cm^{-1} for the silver wire, while 270cm^{-1} for the growing silver nanoparticles. Table 2 shows the signals assignation.

The Raman spectra of the reaction mixture are plotted in Fig. 3. This behavior was attributed to an intermediate step, in which silver carboxylates could be formed; this is thought to be because the symmetric strong COO stretch band is usually seen at 1450-1360cm^{-1} [28]. The symmetric stretching vibrations of C=O groups could be identified at 1658cm^{-1}; from 2 to 10 minutes its intensity remained almost the same, but later, the peak became more intense, indicating that more C=O groups were formed due to the oxidation of 1-octanol to octanoic acid (Caprylic acid). Oleylamine can

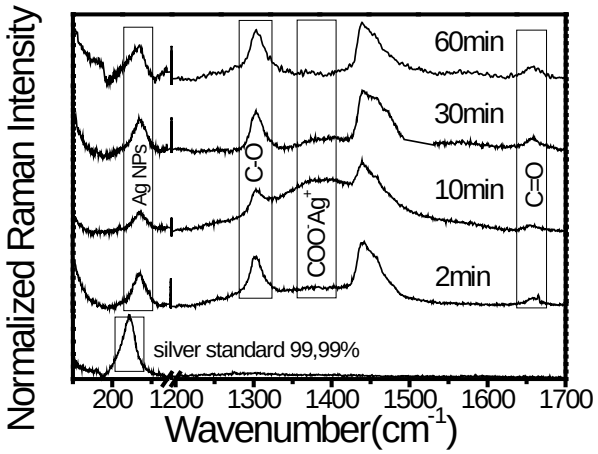

Figure 3. Spectra of the Ag2 reaction mixture.
Source: The authors

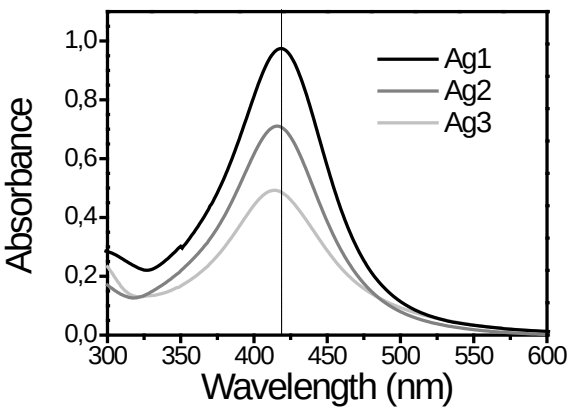

Figure 5. UV-Vis absorption spectra of silver nanoparticles in hexane after purification.
Source: The authors

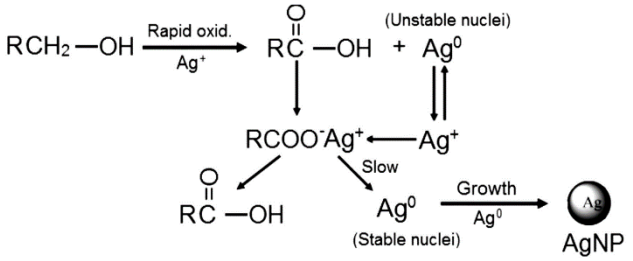

Figure 4. Schematic illustration of the proposed formation mechanism of silver nanoparticles obtained by 1-octanol as reducing agent.
Source: The authors

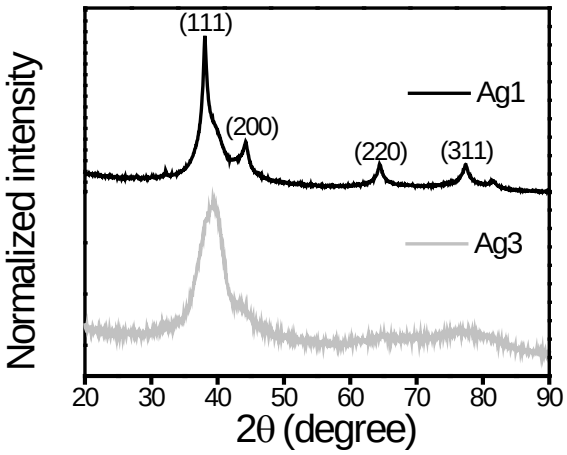

Figure 6. X-ray diffraction patterns of Ag1 and Ag3 silver nanoparticles
Source: The authors

also act as reducing agent and undergo metal-ion-induced oxidation to nitriles [29], but it was not possible to observe changes because the content of Oleylamine was relatively low.

Fig. 4 shows the proposed formation mechanism of silver nanoparticles according to the results observed by Raman. The formation of intermediated unstable silver nanoparticles occurs very rapidly (less than two minutes) as observed in the absorption spectra. These nanoparticles are not large enough to grow and these unstable nuclei can be partially dissolved, and therefore as shown in the Raman results, the peak intensity attributed to the already formed nanoparticles decreased while the silver carboxylate increased (see Fig. 3 at 10 minutes) [24]. As the silver carboxylate formation is an intermediate step, and as the salts are not very stable at 180 °C, they provide the Ag+ ions, which are later reduced to form stable nuclei for the nanoparticles. This means that the formed carboxylates tend to disappear (as seen in the Raman spectrum at 30 minutes) and the intensity associated to the formed nanoparticles has to increase.

Fig. 5 shows the resulting absorbance spectra for the three sets of nanoparticles synthesized in this work. If the particle size becomes comparable to or smaller than the mean free path of the conduction band electrons or "free" electrons, the collisions of the electrons with the particle surface becomes important and the effective mean free path is less than that existing in bulk materials. This usually results in broadening and blue-shift of the plasmon band for particles smaller than about 10 nm [30]. There was a slightly blue shift in the maximum absorbance peak from Ag1 to Ag3. These results suggest that smaller nanoparticles were obtained by increasing the oleic acid concentration, probably because of the steric effects; the growing particles are rapidly capped or stabilized by the molecules of the acid and therefore the opportunity for a particle to interact with others becomes lower.

3.2. Particle size: XRD and TEM

The X-ray diffraction patterns of Ag1 and Ag3 samples are shown in Fig. 6. The peaks of Ag1 perfectly match the face-centered cubic (fcc) structure of the bulk silver, with the broad peaks around 2θ = 38°, 44°, 65°, and 78° corresponding to (111), (200), (220) and (311) lattice planes, respectively.

The average crystallite size of both samples were calculated over the (111) reflection plane using the classical Scherrer Eq.1 [31]. k is the Scherrer constant (k = 0.89) λ is the wavelength of the X-ray, β is the FWHM of the peak and θ is half of the Bragg angle.

$$D = \frac{k\lambda}{\beta \cos\theta} \quad (1)$$

The calculated crystallite size was found to be 5.97nm and 2.63nm for Ag1 and Ag3, respectively. These results are consistent with the absorbance spectra of Fig. 5.

Fig.s 7 and 8 show TEM images of the samples. The corresponding histogram of the particles size distribution for the respective samples is presented along with the TEM images. Ag1 (Fig. 7) ranged from 4 to 71nm and Ag3 from 2.1 to 4.7nm, the latter being more uniform and smaller than Ag1, with an average particle size of 3.8±0.5nm.

A lower concentration of oleic acid resulted in larger crystallites and nanoparticles because it was probably not enough to completely cover the particles' surface and stabilize; therefore, some non-regular shapes (elongated spheres and prisms) were obtained.

According to Fig. 8, there was an important improvement in the distribution of the particles indicating that a simple change in the capping agent's concentration allows for controlling the nanoparticles' shape and size and that can lead to the formation of almost monodispersed nanoparticles

4. Conclusions

Well dispersed silver nanoparticles with controllable size and shape were prepared by reducing silver nitrate with 1-octanol in the presence of oleic acid and oleylamine as capping agents. The nucleation and growth processes could be recognized by UV-vis spectrophotometry. A mechanism for the formation of the silver nanoparticles was proposed according to the Raman measurements, which allowed us to identify that during the reduction of silver ions and oxidation of 1-octanol to caprylic acid, an intermediate step occurred, in which silver carboxylates were formed. Finally, oleic acid limited further aggregation and particle size of silver nanoparticles and fully stabilized the dispersed silver nanoparticles in solution, which served to obtain smaller and more homogenous spherical nanoparticles.

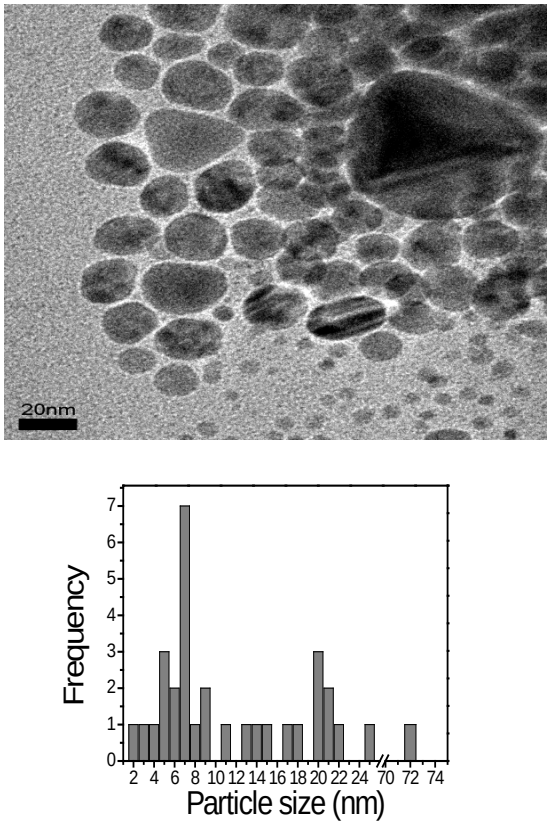

Figure 7. TEM image (top) and the corresponding particle size distribution (bottom) of Ag1.
Source: The authors

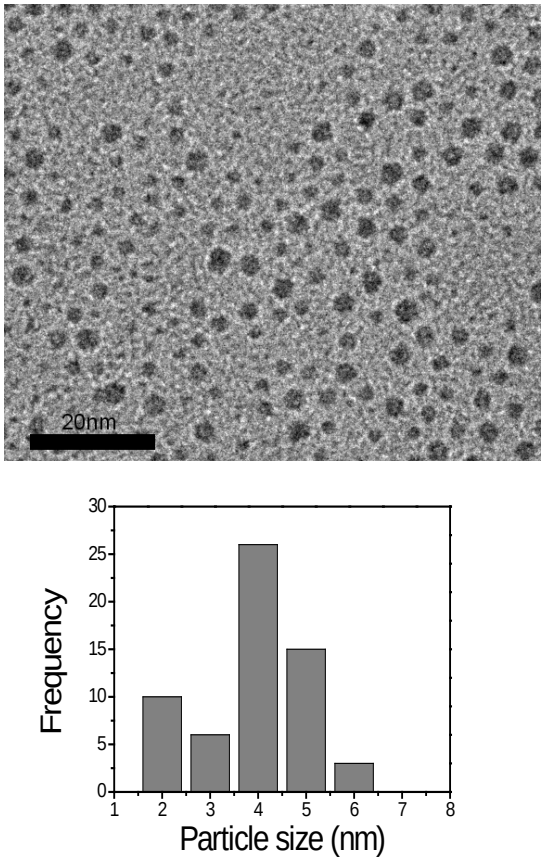

Figure 8. TEM image (top) and the corresponding particle size distribution (bottom) of Ag3.
Source: The authors

Acknowledgements

We would like to thank to *Universidad de Antioquia* for funding this project. Help for TEM characterization from Aditya Baradwaj and Bryan Boudouris from Purdue University is greatly appreciated. The authors also appreciate the support of Harol Torres with the Raman measurements.

References

[1] Tsuboi, A., Nakamura, K. and Kobayashi, N., Chromatic control of multicolor electrochromic device with localized surface plasmon resonance of silver nanoparticles by voltage-step method. Solar Energy Materials and Solar Cells, 145, pp 16-25, 2016. DOI: 10.1016/j.solmat.2015.07.034

[2] Xiangheng, N., Libo, S., Jianming, P., Fengxian, Q., Yongsheng, Y., Hongli, Z., and Minbo, L., Modulating the assembly of sputtered silver nanoparticles on screen-printed carbon electrodes for hydrogen peroxide electroreduction:

Effect of the surface coverage. Electrochimica Acta, 199, pp 187-193, 2016. DOI: 10.1016/j.electacta.2016.03.100

[3] Steffan, M., Jakob, A., Claus, P. and Lang, H., Silica supported silver nanoparticles from a silver (I) carboxylate: Highly active catalyst for regioselective hydrogenation. Catalysis Communications, 10, pp. 437-441, 2009. DOI: 10.1016/j.catcom.2008.10.003

[4] Kalfagiannis, N., Karagiannidis, P.G., Pitsalidis, C., Panagiotopoulos, N.T., Gravalidis, C., Kassavetis, S., Patsalasc, P. and Logothetidisa, S., Plasmonic silver nanoparticles for improved organic solar cells. Solar Energy Materials and Solar Cells, 104, pp 165-174, 2012. DOI: 10.1016/j.solmat.2012.05.018

[5] Pei, J., Tao, J., Zhou, Y., Dong, Q., Liu, Z., Li, Z, Chen, F., Zhang, J., Xu, W. and Tian, W., Efficiency enhancement of polymer solar cells by incorporating a self-assembled layer of silver nanodisks. Solar Energy Materials and Solar Cells, 95, pp. 3281-3286, 2011. DOI: 10.1016/j.solmat.2011.07.007

[6] Kang, Y., Si, M., Zhu, Y., Miao, L. and Xu, G., Surface-enhanced Raman scattering (SERS) spectra of hemoglobin of mouse and rabbit with self-assembled nano-silver film. Spectrochimica Acta Part A: Molecular and Biomolecular Spectroscopy, 108, pp. 177-180, 2013. DOI: 10.1016/j.saa.2013.01.098

[7] Vanamudan, A. and Sudhakar, P.P., Biopolymer capped silver nanoparticles with potential for multifaceted applications. International Journal of Biological Macromolecules, 86, pp. 262-268, 2016. DOI: 10.1016/j.ijbiomac.2016.01.056

[8] Bi, L., Dong, J., Xie, W., Lu, W., Tong, W., Tao, L. and Qian, W., Bimetallic gold–silver nanoplate array as a highly active SERS substrate for detection of streptavidin/biotin assemblies. Analytica Chimica Acta, 805, pp. 95-100, 2013. DOI: 10.1016/j.aca.2013.10.045

[9] Geetha, K., Umadevi, M., Sathe, G.V., Vanelle, P., Terme, T. and Khoumeri, O., Orientation of 1,4-dimethoxy-3–bromomethylanthracence-9,10-dione on silver nanoparticles: SERS studies. Journal of Molecular Structure, 1059, pp. 87-93, 2014. DOI: 10.1016/j.molstruc.2013.11.013

[10] Raza, A. and Saha, B., In situ silver nanoparticles synthesis in agarose film supported on filter paper and its application as highly efficient SERS test stripes. Forensic Science International, 237, 2014.

[11] Chernousova, S. and Epple, M., Silver as antibacterial agent: Ion, nanoparticle, and metal. Angewandte Chemie International Edition, 52, pp. 1636-1653, 2013. DOI: 10.1002/anie.201205923

[12] Chatre, A., Solasa, P., Sakle, S., Thaokar, R. and Mehra, A., Color and surface plasmon effects in nanoparticle systems: Case of silver nanoparticles prepared by microemulsion route. Colloids and Surfaces A: Physicochemical and Engineering Aspects, 404, pp. 83-92, 2012. DOI: 10.1016/J.COLSURFA.2012.04.016

[13] An, W., Zhu, T. and Zhu, Q., Numerical investigation of radiative properties and surface plasmon resonance of silver nanorod dimers on a substrate. Journal of Quantitative Spectroscopy and Radiative Transfer, 132, pp. 28-35, 2014. DOI: 10.1016/j.jqsrt.2013.01.013

[14] Mehta, S.K., Chaudhary, S. and Gradzielski, M., Time dependence of nucleation and growth of silver nanoparticles generated by sugar reduction in micellar media. Journal of Colloid and Interface Science, 343, pp. 447-453, 2010. DOI: 0.1016/j.jcis.2009.11.053

[15] Saion, E., Gharibshahi, E. and Naghavi, K., Size-Controlled and optical properties of monodispersed silver nanoparticles synthesized by the radiolytic reduction method. International Journal of Molecular Sciences, 14, pp. 7880-7896, 2013. DOI: 10.1021/la0600245

[16] Shin, H.S., Yang, H.J., Kim, S.B. and Lee, M.S., Mechanism of growth of colloidal silver nanoparticles stabilized by polyvinyl pyrrolidone in γ-irradiated silver nitrate solution. Journal of Colloid and Interface Science, 274, pp. 89-94, 2004. DOI: 10.1016/J.JCIS.2004.02.084

[17] Dadosh, T. Synthesis of uniform silver nanoparticles with a controllable size. Materials Letters, 63, pp. 2236-2238, 2009. DOI: 10.1016/J.MATLET.2009.07.042

[18] Yamamoto, M., Kashiwagi, Y. and Nakamoto, M., Size-controlled synthesis of monodispersed silver nanoparticles capped by long-chain alkyl carboxylates from silver carboxylate and tertiary amine. Langmuir, 22, pp. 8581-8586, 2006. DOI: 10.1021/LA0600245

[19] Chiang, I.C., Chen, Y.T. and Chen, D.H., Synthesis of NiAu colloidal nanocrystals with kinetically tunable properties. Journal of Alloys and Compounds, 468, pp. 237-245, 2009. DOI: 10.1016/J.JALLCOM.2008.01.063

[20] Li, Y., Zhang, X.L., Qiu, R. and Kang, Y.S., Synthesis and investigation of SmCo5 magnetic nanoparticles. Colloids and Surfaces A: Physicochemical and Engineering Aspects, 313, pp. 621-624, 2008. DOI: 10.1016/J.COLSURFA.2007.04.150

[21] Chen, M., Feng, Y.G., Wang, X., Li, T.C., Zhang, J.Y., and Qian, D.J., Silver nanoparticles capped by oleylamine: Formation, growth, and self-organization. Langmuir, 23, pp. 5296-5304, 2007. DOI: 10.1021/LA700553D

[22] Chen, Y., Gao, N. and Jiang, J., Surface matters: Enhanced bactericidal property of core–shell Ag–Fe2O3 nanostructures to their heteromer counterparts from one-pot synthesis. Small, 9, pp. 3242-3246, 2013. DOI: 10.1002/SMLL.201300543

[23] Jana, N.R., Sau, T.K. and Pal, T., Growing small silver particle as redox catalyst. The Journal of Physical Chemistry B, 103, pp. 115-121, 1998. DOI:10.1021/JP982731F

[24] Lamer, V.K. and Dinegar, R.H., Theory, production and mechanism of formation of monodispersed hydrosols. Journal of the American Chemical Society, 72, pp. 847-854, 1950. DOI: 10.1021/ja01167a001

[25] Goia, D.V., Preparation and formation mechanisms of uniform metallic particles in homogeneous solutions. Journal of Materials Chemistry, 14, pp. 451-458, 2004. DOI: 10.1039/B311076A

[26] Harada, M, Inada, Y. and Nomura, M., In situ time-resolved XAFS analysis of silver particle formation by photoreduction in polymer solutions. Journal of Colloid and Interface Science, 337, pp. 427-438, 2009. DOI: 10.1016/j.jcis.2009.05.035

[27] Martina, I., Wiesinger, R., Jembrih, D. and Schreiner, M., Micro-raman characterisation of silver corrosion products: Instrumental set up and reference database. E-Preservation Science: Morana RTD [Online]. pp. 1-8, 2012. Available at: http://www.morana-rtd.com/e-preservationscience/2012/Martina-05-03-2012.pdf

[28] Lin-Vien, D., Colthup, N. B., Fateley, W.G. and Grasselli, J.G., CHAPTER 9 - Compounds containing the carbonyl group. In: Lin-Vien, D, Colthup, NB, Fateley, WG, Grasselli, JG, eds. The Handbook of Infrared and Raman Characteristic Frequencies of Organic Molecules. San Diego: Academic Press, 1991, pp. 117-154.

[29] Mourdikoudis, S. and Liz-Marzán, L.M., Oleylamine in nanoparticle synthesis. Chemistry of Materials, 25, pp. 1465-1476, 2013. DOI: 10.1021/cm4000476

[30] Zhang, J.Z., Optical Properties and Spectroscopy of Nanomaterials. Cahpter 7 - Optical Properties and Spectroscopy of Nanomaterials: World Scientific, 2009, pp. 205-235.

[31] Scherrer, P., Bestimmung der Grösse und der inneren Struktur von Kolloidteilchen mittels Röntgenstrahlen. [Online]. pp. 98-100, 1918. Available at: http://gdz.sub.uni-goettingen.de/dms/load/img/?PPN=GDZPPN002505045&IDDOC=63709

D. Ramirez, is currently a PhD student in Materials Engineering at Universidad de Antioquia, Medellín, Colombia, where he also completed his BSc. Eng in Materials Engineering in 2014. His research interests include nanothecnology and nanostructured solar cells. He is currently working on synthesis and characterization of nanoparticles, nanocomposites and novel semiconductors for thin film photovoltaic applications in The Center of Research, Innovation and Development of Materials – CIDEMAT at Universidad de Antioquia.
ORCID: 0000-0003-2630-7628

F. Jaramillo, completed his BSc. Eng in Chemical Engineering at Universidad de Antioquia, Medellín, Colombia, in 2001 and, in 2005, a PhD in Chemistry at The University of Manchester, USA. He is the current director of the solar cells lab EPM-UdeA, part of the Nanotechnology Regional Iniciative at Ruta N-Medellín, and a member of the national advisory council in Nanoscience and Nanotechnology - Red NanoColombia. His research interest areas include nanotechnology, nanostructured solar cells, novel semiconductors, energy materials, nanocomposites, and functional polymers from renewable resources. He is currently an associated professor at Materials Engineering Department and member of The Center of Research, Innovation and Development of Materials – CIDEMAT at Universidad de Antioquia.
ORCID: 0000-0003-1722-5487